Paper-Based Pump-Free Magnetophoresis

SCHOLARONE™
Manuscripts

Paper-Based Pump-Free Magnetophoresis

Zachary D. Call[1], Cody S. Carrell[1], Ilhoon Jang[1,2], Brian J. Geiss[4,5], David S. Dandy[3,4], Charles S. Henry[1,4][*]

[1]Department of Chemistry, Colorado State University, Fort Collins, CO 80523, USA
[2]Institute of Nano Science and Technology, Hanyang University, Seoul 04763, Korea
[3]Department of Chemical and Biological Engineering, Colorado State University, Fort Collins, CO 80523 USA
[4]School of Biomedical Engineering, Colorado State University, Fort Collins, CO 80523, USA
[5]Department of Microbiology, Immunology, and Pathology, Colorado State University, Fort Collins, CO 80523, USA

*Corresponding author: Chuck.Henry@colostate.edu

Abstract

Microfluidic magnetophoresis is a powerful technique that is used to separate and/or isolate cells of interest from complex matrices for analysis. However, mechanical pumps are required to drive flow, limiting portability and making translation to point-of-care (POC) settings difficult. Microfluidic paper-based analytical devices (µPADs) offer an alternative to traditional microfluidic devices that do not require external pumps to generate flow. However, µPADs are not typically used for particle analysis because most particles become trapped in the porous fiber network. Here we report the ability of newly developed fast-flow microfluidic paper-based analytical devices (ffPADs) to perform magnetophoresis. ffPADs use capillary action in a gap between stacked layers of paper and transparency sheets to drive flow at higher velocities than traditional µPADs. The multi-layer ffPADs allow particles and cells to move through the gap without being trapped in the paper layers. We first demonstrate that ffPADs enable magnetic particle separations in a µPAD with a neodymium permanent magnet and study key factors that affect performance. To demonstrate utility, *E. coli* was used as a model analyte and was isolated from human urine before detection with a fluorescently labeled antibody. A capture efficiency of 61.5% was then obtained of *E. coli* labeled magnetic beads in human urine. Future studies will look at the improvement of the capture efficiency and to make this assay completely off-chip without the need of a fluorescent label. The assay and device described here demonstrate the first example of magnetophoresis in a paper based, pump free microfluidic device.

1. Introduction

Improving medical diagnostics is a key need to reduce the 15 million deaths a year from infectious diseases.[1] While significant improvement has been made in the field, patients in many parts of the world still cannot access early diagnosis which is crucial for adequate care.[2-5] For example, sepsis patients treated within one day of showing symptoms had a 10% mortality rate, while those treated after three days had a 50% mortality rate.[6] Current infectious disease detection methods include culturing, polymerase chain reaction (PCR), and enzyme-linked immunosorbent assay (ELISA).[1, 7] These methods are widely accepted because of their ability to detect bacteria with low limits of detection.[8-10] However, all require trained personnel, can take days to weeks to complete, and cost at least $10 per test.[11] Consequently, a simple, rapid, and reliable point-of-care (POC) diagnostic for the detection of infectious diseases that is both sensitive and selective is needed. Land et al. recently recommended POC technologies to meet a REASSURED criteria.[12] These criteria are defined as real-time connectivity, ease of specimen collection, affordable, sensitive, specific, user-friendly, rapid and robust, and equipment-free. µPADs are one technology that meets many of these requirements but suffers from slow fluid velocity and poor limits of detection.[2, 13] One technique known to improve detection limits and selectivity of an assay is to separate target analytes from the sample matrix.[14]

In this work, we are focused on isolating bacteria from complex matrices to remove interferents, concentrate the target cells, and improve detection performance. The cell separation/isolation process can be tedious, so microfluidic platforms have been developed to automate and simplify this process.[15] A popular microfluidic separation approach is magnetophoresis, which separates cells in continuous flow using a permanent magnet to move magnetically labeled cells from one flowing stream to another.[16] However, magnetophoresis requires external pumps to drive flow, limiting their portability and usefulness for POC applications. µPADs transport fluid via capillary action, which eliminates the need for external pumps,[17] but are not currently used for magnetophoresis because particles and cells become trapped in the paper fibers and fluid velocities generated in µPADs are not fast enough for continuous separation.[18] In this work we

solve both issues by creating fast flow in a modified multi-layer μPAD.[2, 13, 19-21] Fast-flow μPADs (ffPADs) are created by stacking two layers of wax-printed paper around laser cut double sided adhesive to create channels or gaps. The channels between paper layers enable fast flow without trapping particles. The velocities in the multi-layer µPAD increase by 145× or more compared to single-layer µPADs. The fast-flow phenomenon seen with this method of fabrication was characterized in depth previously in Channon *et al.*[19, 20] Taking advantage of this fast-flow phenomenon provides a way to make paper-based magnetophoresis possible.[19] Herein we describe the first example of a paper-based, pump-free magnetophoretic device and demonstrate its capabilities by detecting bacteria in urine. We envision the µPAD designed here for rapid detection of *E. coli* and other bacteria and viruses would benefit both food safety and human health diagnostics.

2. Materials and Methods

2.1 Materials.

Whatman 1 chromatrography paper was purchased from GE Healthcare Sciences. Wax patterns were printed using a Xerox ColorQube 8870 and an IsoTemp hot plate (Fisher Scientific) was used to melt the wax. A benchtop digital microscope (Dino-Lite AF4915) was used for laminar flow colorimetric experiements. Two fluorescent Dino-Lite digital microscopes with exictation wavelengths of 400 nm and 570 nm (Dino-Lite AM4115T-CFVW and Dino-Lite AM4115T-YFGW) were used for fluorescence detection and analysis. All videos were imported into ImageJ for analysis. A cynlindrical ¼" x ¼" Neodymium Iron Boron (NdFeB) permanent magnet, grade N52 (K&J Mangetics, INC.) was used to create an external magnetic field. Other magnet types and shapes were investigated, however the cynlindrical magnet was choosen because of the smaller size while maintaining strong field lines. All magentic beads were purchased from Spherotech Inc. (Lake Forest, Illnois). *E. coli* antibodies (bs-2033R/bs-2033R-A555) were purchased from Bioss Antibodies. The buffers used in this work were 0.1 M phosphate-buffered saline (PBS) and

0.1 M PBS with 0.1% Tween-20 (PBST). The two antibodies were diluted in PBS. Human pooled

urine was purchaed from Lee Biosolutions (Maryland Heights, MO).

2.2 Device Design and Fabrication.

The µPADs discussed here were designed in CorelDRAW X4 and then printed onto Whatman

grade 1 chromatography paper and a cellulose acetate transparency sheet (3M PP2950). Next

the paper was placed on a hot plate at 150°C for 90 s to create hydrophobic barriers. Grade 467

and 468 double-sided adhesive were used to define the gap height, and the channel pattern was

cut out using a CO_2 laser cutter (Epilog Zing Laser Cutter and Engraver). The multilayered device

was then assembled in 8.5"×11" sheets by first applying the double-sided adhesive to the

transparency and applying consistent pressure with a pouch laminator set at room temperature.

Next, the top paper layer was placed directly onto the double-sided adhesive using a guide to

provide necessary alignment to create the ffPAD.

2.3 Magnetophoresis System Setup.

A range of fluorescent carboxyl magnetic particles from 2.0 µm to 44.1 µm were purchased

from Spherotech Inc. and diluted from 5 mg/mL to 1 mg/mL in phosphate buffered saline (PBS).

All 44.1 µm particles used in these and following studies were labeled with a yellow fluorophore

onto the surface of the particles with an excitation wavelength from 400-500 nm and emission

from 450-550 nm. Imaging was done with the Dino-Lite microscope (400 nm). All dilutions of

particles were made in phosphate-buffered saline, pH 7.2, kept at room temperature and

protected from light. Solutions were vortexed for 30 s before use (Scientific Industries Vortex

Genie 2). The Grade N52 permanent magnet was placed on top of the device and placement

was optimized for consistent and ideal separation results based on magnetic field lines. Images

of the fluorescent particles within the gap of the device were taken using the fluorescent DinoLite

microscope.

2.4 *E. coli* Growth and Sample Preparation.

E. coli DH5-α was used as the model bacteria in this work; it was grown in Universal Pre-Enrichment Broth (Sigma-Aldrich, pH 7) overnight in a shaker at 37°C and 220 rpm. The bacteria concentration was quantified by serial dilution and plating on lysogeny broth (LB) agar plates. Serial dilutions of this soltuion were made using PBS or human pooled urine.

2.5 *E. coli* Detection Using Immunomagnetic Separation and H-Cell Device in Human Urine.

The enzymatic assay presented by Srisa-Art et al. was modified for DH5-α detection.[22] The entire assay was perfromed on the benchtop at room temperature. First, 44.1 μm streptavidin-coated paramagnetic beads (SpheroTech) were vortexed for 30 s at room temperature. Second, the beads were conjugated to a biotinylated anti-*E. coli* antibody in a microcentrifuge for 20 min on a rotator. Third, an immunomagnetic separation (IMS) was performed using a magnet (DynaMag-2 magnet, Thermo Fisher Scientific, Inc.) to isolate and concentrate the magnetic bead-antibody complex by removing the supernatant and resuspending the content in 100 μL of PBS. Fourth, the bead-antibody complex was added to 1 mL of *E. coli* spiked urine and incubated on a rotator for 20 min. Another IMS step was performed to isolate/concentrate the sample and to remove the supernatant. The complex was washed twice with PBS-Tween (0.1%) to remove any unbound species. Finally, an anti-*E. coli* AlexaFluor-555 was conjugated to the bead complex for 20 min on a rotator. The final complex was then washed twice using IMS with PBS-Tween. The complex was then resuspended in 50 μL of urine. 30 μL of the complex was then added simulatenoulsy to the device with 30 μL of PBS buffer to create capillary driven laminar flow. The permanet magnet was placed on the adjacent channel at the desired detection zone. After 30 s the fast-flow has stopped and analysis of *E. coli* capture was performed.

2.6 Image Analysis.

Videos of all experiments were taken with the DinoLite microscopes and pictures were then exported to be analyzed in NIH ImageJ. The images were split into red, green, and blue channels for elimination of background signal and analysis. Fluorescence intensity plots were created with proportional mean grey scale values.

3. Results and Discussion

3.1 Device Dimensions and Laminar Flow.

An H-cell device was created from paper and transparency film to demonstrate capillary driven laminar flow was possible. The device was assembled by stacking packing tape, paper, double-sided adhesive, transparency together as shown in **Fig.1a**. **Fig. 1b** shows the cross-sectional view of the channel once the device is assembled. ffPADs yield faster sustained flows than traditional µPADs, as demonstrated in **Fig. 1c** where the liquid 6 cm from the inlet in a ffPAD with 360 µm gap has a speed of 0.62 cm/s versus 0.0035 cm/s in traditional single-layer µPAD.[19] The gap height can be controlled by changing the number of double-sided adhesive layers placed between the paper and transparency layers. Modeling of this phenomenon recently published by Channon *et al.* describes flow dominated by Laplace pressure for the first 1-2 cm.[20] Shown by a still image in the supplemental, the fluid flow in the gap of the device is dragging the liquid in the paper layer. The flow in the gap is then dominated by a "moving wall" of liquid, resulting in a shear flow within the paper and a linear velocity profile.[19, 20] The modeling described is confirmed by the experimental results in **Fig. 1c** where there are fast initial velocities of over 4 cm/s for a 360 µm gap height that decay over time.[20] The fluid velocities in the devices shown here have similar flow characteristics and show the same experimental results described by Channon *et al.*[19, 20] Although ffPADs have shown faster velocities when compared to traditional µPADs, the maximum Reynolds number (*Re*) in the multi-layer device

was calculated to be 2.0, which occurred in the 360 μm gap configuration, confirming that flow is extremely laminar. Based on the studies showing sustained high velocities, we were led to hypothesize that magnetophoresis was possible because ffPADs have a large enough gap height for the majority of suspended particles to avoid being trapped in the cellulose fibers.[4, 19, 23]

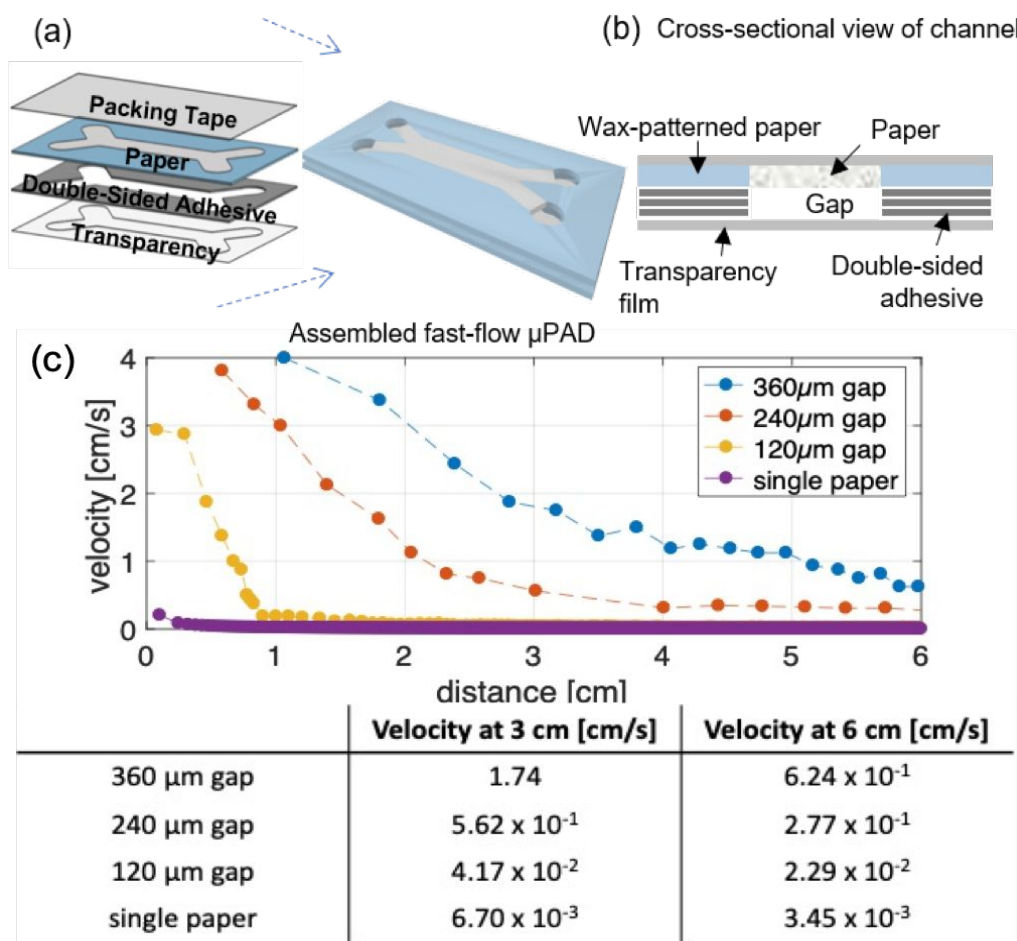|	Velocity at 3 cm [cm/s]	Velocity at 6 cm [cm/s]
360 μm gap	1.74	6.24×10^{-1}
240 μm gap	5.62×10^{-1}	2.77×10^{-1}
120 μm gap	4.17×10^{-2}	2.29×10^{-2}
single paper	6.70×10^{-3}	3.45×10^{-3}

Fig. 1 Assembly and flow characteristics of microfluidic paper-based analytical devices (μPADs) (a) Schematic of fast-flow μPAD assembly. (b) Cross-sectional view of channel of fast flow μPADs, with flow to-ward/away from the observer. (c) Plot showing flow velocities with respect to gap height.

We next sought to demonstrate laminar flow in the ffPAD configuration because consistent laminar flow is needed for magnetophoresis to avoid convective mixing between the two parallel flowing streams in the H-cell.[24] A ffPAD with two inlets containing red and green dyes showed a clear interface between the two liquid streams, again confirming laminar flow was established in the device with only slight diffuisonal mixing (**Fig. 2a**). Following the demonstration of fully developed laminar flow, the effect of inlet angle was quantified using the absolute mixing index

(AMI) as a measure of total mixing. AMI indicates the extent of mixing and operates on a scale of 0-1, where 0 indicates a completely mixed state and 1 indicates a completely unmixed state. Photographs above each gragh in **Fig. 2b** show each device and the main channel where the analysis is performed. Devices I, II, and III were all consistent with a 3 mm wide channel with only changing the angle of the inlet. Where device I had a 90˚ angle, device II had a 180˚ angle and device III had a 15˚ angle. Devices I and II showed inconsistent flow with relativley large standard deviation of ±1 shown in blue. In device III a 15° angle between the two inlets led to less mixing and more reproducible laminar flow. Device IV was fabricated incorporating the optimal angle geometry with a 270° fan at end of the channels that produces steady flow in paper analytical devices.[21, 25] Inserting the fan decreased variability and increased AMI (**Fig. 2b).** Device IV showed the most reproducible laminar flow along with the least mixing denoted by an AMI of 0.7 with only diffusional mixing occuring. As a result, the Device IV geometry was selected for subsequent studies.
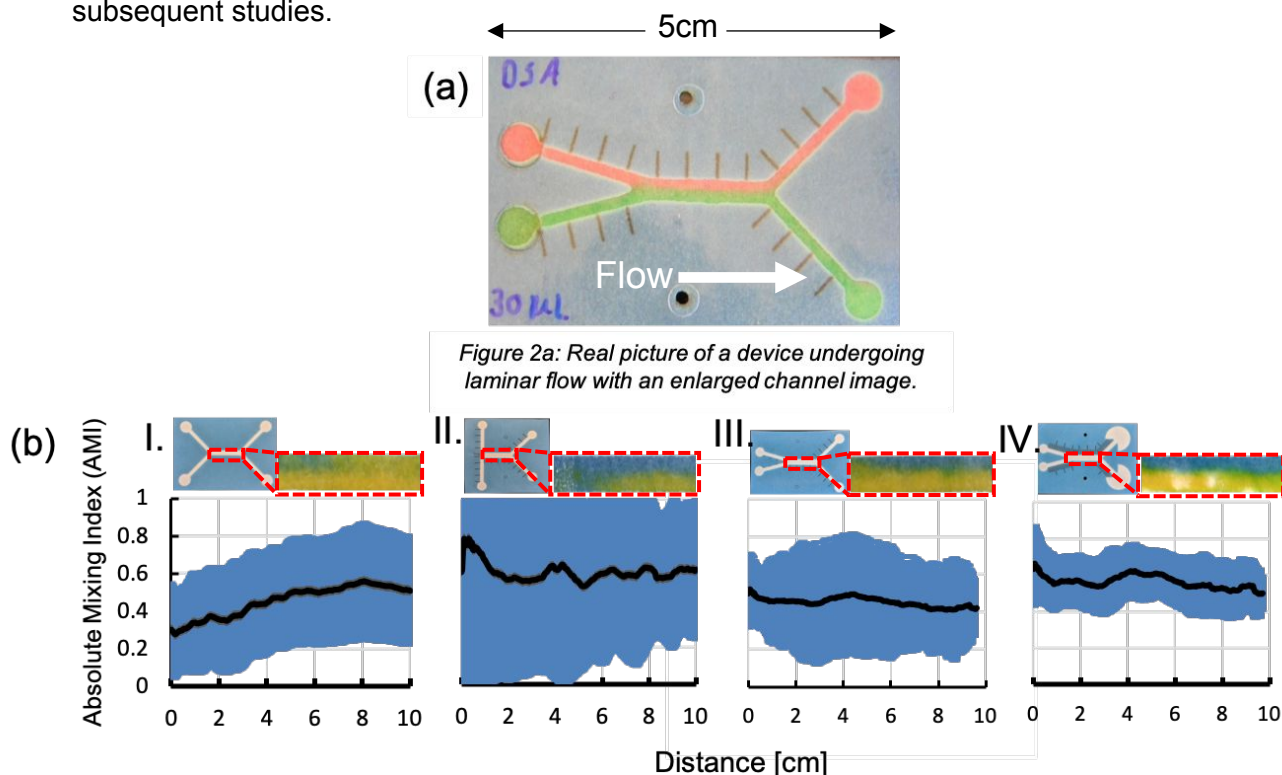

Figure 2a: Real picture of a device undergoing laminar flow with an enlarged channel image.

***Fig 2.** (a) Image taken of fast-flow µPAD with laminar flow. (b) Images taken of the middle channel to analyze AMI. The corresponding graphs show the effect the angle has on consistency of laminar flow by quantifying the amount of mixing of each device.*

3.2 Understanding Particle Behavior.

Once velocities and laminar flow parameters were characterized, particle separation via magnetophoresis was investigated. Since the bottom layer of the ffPADs was made from transparency film, it was possible to image the magnetic particles inside the gap. **Fig. 3a** shows a qualitative schematic of expected particle trajectories, where magnetic particles move across the laminar flow interface and are trapped by a permanent magnet. The NdFeB permanent magnet was placed on the top side of the device on the edge of the channel. 2 μm, 8 μm, and 44.1 μm magnetic particles were tested. The sizes were selected based on commercial availability. 2 μm and 8 μm particles were retained within the paper fibers resulting in no observable movement across the parallel flowing streams and significant fluorescent background in the channel (**Figs. 3b and 3c**). Whatman 1 chromatography paper has an average pore size of 11 μm, which resulted in trapping particles size smaller than 11 μm in the device. In addition to particle size, the magnetic susceptibility changes proportionally with the size of the particles. As a result, the 44.1 μm particles remained in the gap area between paper and transparency film and could be moved across the laminar flow barrier with ease (**Fig. 3d**). The 44.1 μm magnetic particles also accumulated near the magnet. As a control, the trajectories of the 44.1 μm particles were obtained in the absence of a magnetic field. Without the field present the particles largely followed the liquid streamlines and did not cross the parallel streams' interface (**Fig. 3e**). The flow velocities of the particles follow velocities shown in **Fig. 1c**. The ability to pull the 44.1 μm particles from one stream to another with the magnetic field under continuous flow is the first time magnetophoresis has been demonstrated in a pump-free device to the best of our knowledge.

After confirming magnetophoresis in ffPADs, the concentration dependent signal was evaluated by analyzing the fluorescence intensity of captured particles by taking the mean grey scale intensity of the area at magnet. **Fig. 3f** shows the normalized fluorescence intensity variation as a function of particle concentration. The linear calibration curve shows the fluorescent

signal increasing with increasing particle concentration with corresponding error bars taken from

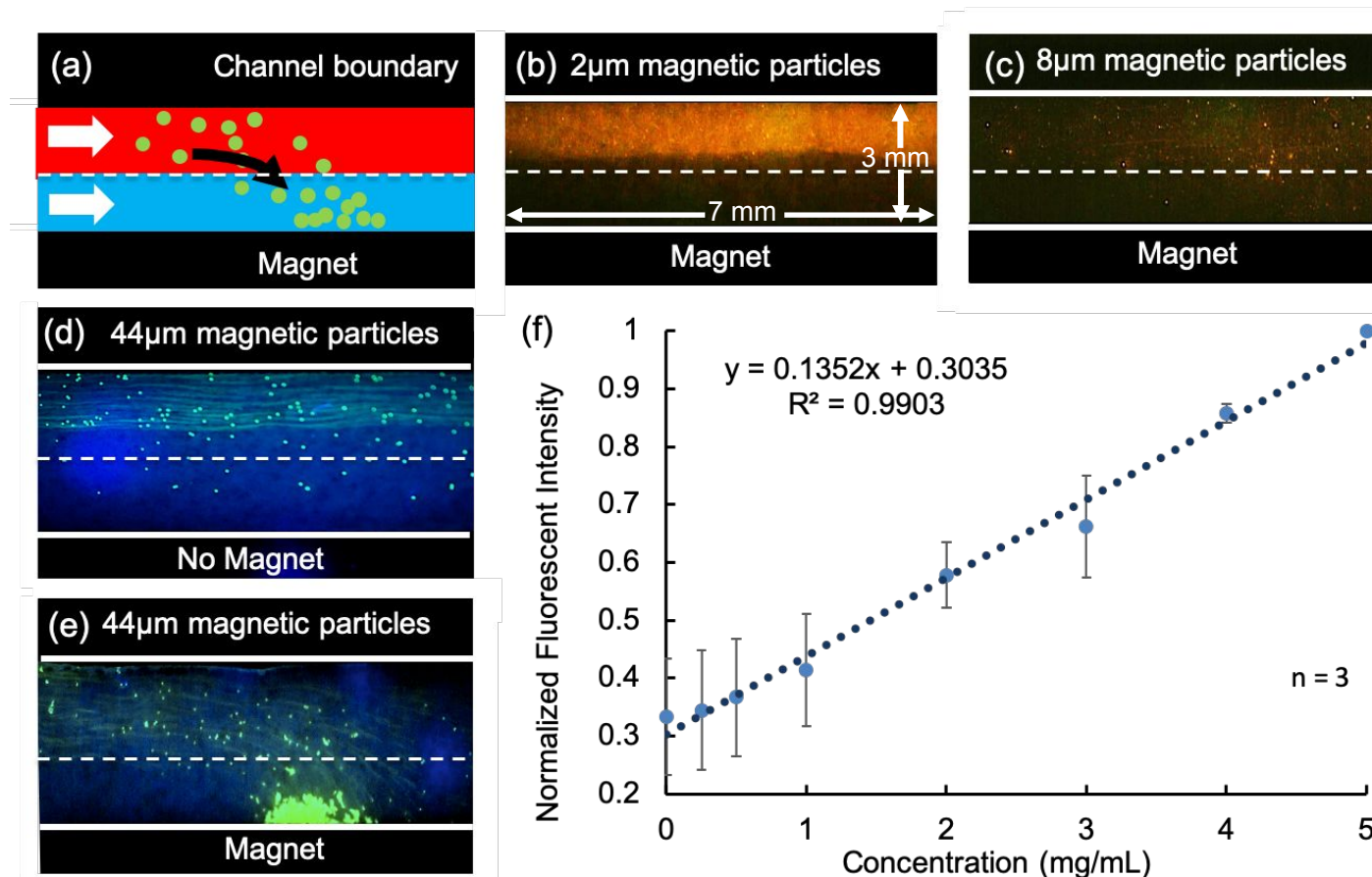a standard deviation with an n of 3 for each concentration.

Fig 3. Magnetophoresis in microfluidic paper-based analytical devices (μPADs) (a) Overview of magnetophoresis concept, where the white-dashed lines are the laminar flow interface (b) 2μm magnetic particles in device (c) 8μm magnetic particles in device (d) Control image of particles following streamlines in the absence of a magnetic field. (e) 44μm magnetic particles undergoing positive magnetophoresis (f) Calibration curve of fluorescent intensity of particle capture via concentration.
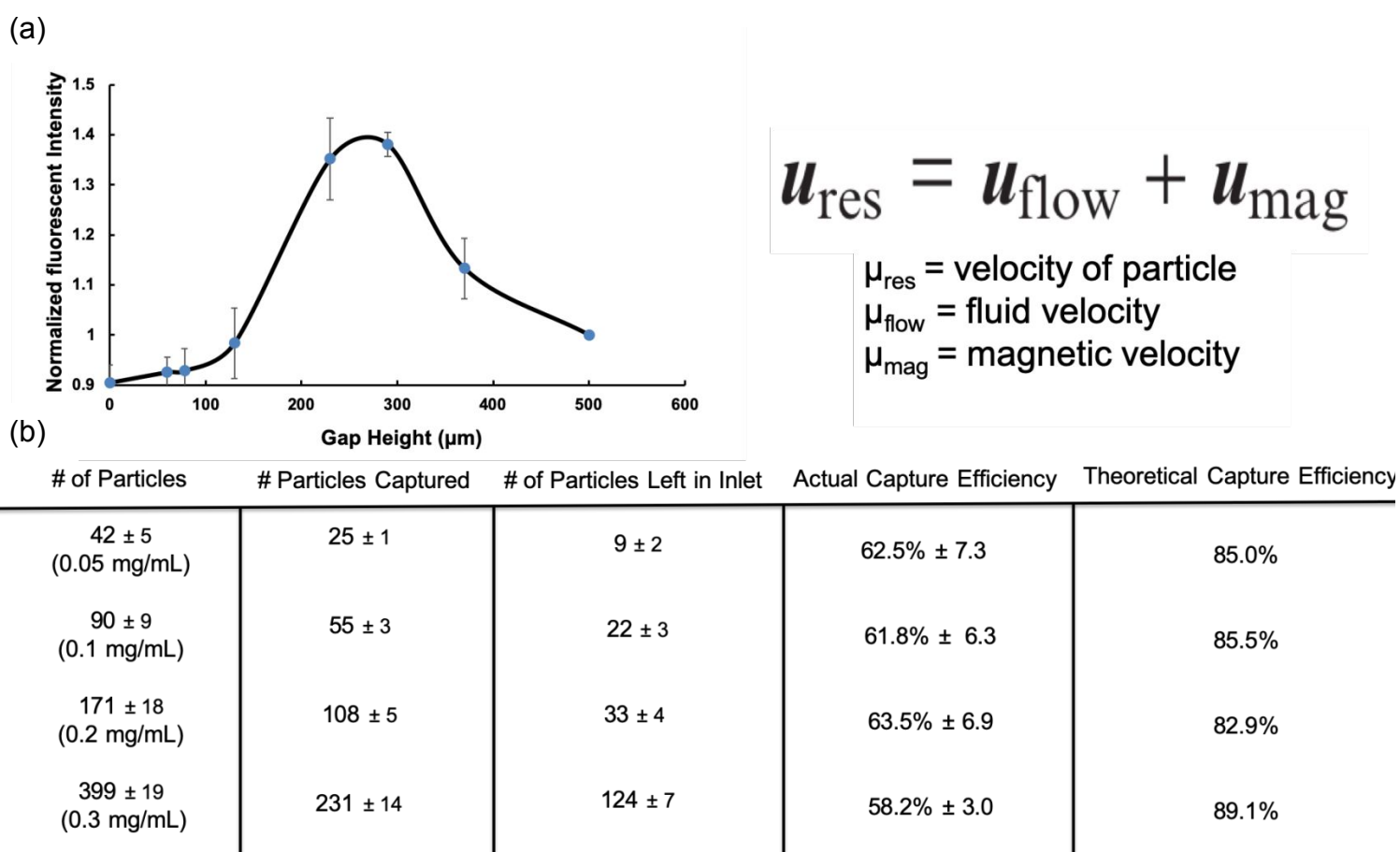
3.3 Improvements in Device Design.

The effect of gap height on particle capture was investigated. Pamme et al. showed in a glass

microchip that if fluid velocities are above 0.2 cm/s then little to no deflection of magnetic particles

occurs. Conversely, if velocities are lower than 0.04 cm/s the magnetic moment will be more

pronounced and inherently influence the particle deflection trajectory.[26] Since the velocity and

magnetic field vectors are orthogonal, faster flow decreases particle deflection caused by a

constant magnetic field, as described by the equation shown in **Fig. 4**. The fluid velocity in a ffPAD

is controlled by the gap height between the layers, so the gap height was varied to study these competing effects.[19] ffPAD gap heights of 60, 70, 120, 230, 290, 360, and 500 μm were tested using 44.1 μm magnetic particles and the fluorescent intensity of captured particles analyzed. A gap height between 230 and 290 μm yielded the highest number of magnetic particles captured by the magnet (**Fig. 4a).** In the ffPAD, a velocity exceeding ~1.5 cm/s prevented the particles from being captured. When the velocity was lower than ~0.5 cm/s the particles were retained in the paper fibers particle accumulation at the magnet was not observed.

In addition to optimizing gap height, the shapes of the outlet channels were studied. The magnetic particles follow a curved deflection trajectory. To account for this trajectory and improve the efficiency of particle capture, the device design was modified to match the general shape of the trajectory. A thin wax line was also printed on the top paper layer directly down the center of the channel to improve flow reproducibility. The particles then deflect only in the gap of the device and mixing in the paper is minimized. Additionally, a larger fan with a 14 mm diameter was used with the upper channel versus a 9.5 mm diameter fan on the lower channel. The larger fan is used to continually wick the solution from the upper channel and particle inlet to transport more particles to the detection zone and improve capture efficiency (**Fig. 5)**. The magnetic field is shown with an overlay of a schematic of the device and magnetic particles following the field lines and being attracted toward the high gradient. The shape of the outlet channels were designed to match that of the magnet field lines to further improve capture of the magnetic particles. [27] After optimization of the device was completed the capture efficiency was then investigated yielding capture of 61.5% ± 5.8 (n=4) with similar efficiencies for increasing concentrations. Other studies have shown capture efficiencies anywhere from 44% to 100% with permanent magnets, however all previous studies were conducted in traditional microfluidic channels using pumps.[28] Concentrations from 0.05 mg/mL to 0.3 mg/mL were selected because of the ability to physically count the number of particles in a 30 μL sample. The lowest capture was reported for the highest concentration because particles will aggregate at higher concentrations. The calculated capture

1
2
3   efficiency of 61.5% was further analyzed and it was determined that many of the large 44.1μm
4
5   particles sediment to the bottom of the inlet and are trapped before reaching the capture magnet.
6
7   If the particles left in the inlet were able to reach the capture zone, a theoretical yield of 85.6%
8
9   would result (**Fig 4c)**. This is calculated by counting the number of particles left in the inlet versus
10
11   the total number of particles added (n=4). A washing step of buffer immediately after the initial
12
13   addition showed an increase of ~5%.
14
15
16
17
18   (a)
19

$$u_{res} = u_{flow} + u_{mag}$$

μ_{res} = velocity of particle
μ_{flow} = fluid velocity
μ_{mag} = magnetic velocity

(b)

# of Particles	# Particles Captured	# of Particles Left in Inlet	Actual Capture Efficiency	Theoretical Capture Efficiency
42 ± 5 (0.05 mg/mL)	25 ± 1	9 ± 2	62.5% ± 7.3	85.0%
90 ± 9 (0.1 mg/mL)	55 ± 3	22 ± 3	61.8% ± 6.3	85.5%
171 ± 18 (0.2 mg/mL)	108 ± 5	33 ± 4	63.5% ± 6.9	82.9%
399 ± 19 (0.3 mg/mL)	231 ± 14	124 ± 7	58.2% ± 3.0	89.1%

Fig. 4 (a) Optimization of particle capture with respect to gap height characterized by fluorescent intensity with correlated equation showing the relationship of the velocity of the particle with respect to the fluid and magnetic velocity. (b) Actual and theoretical capture efficiency in the device with an optimized gap height.
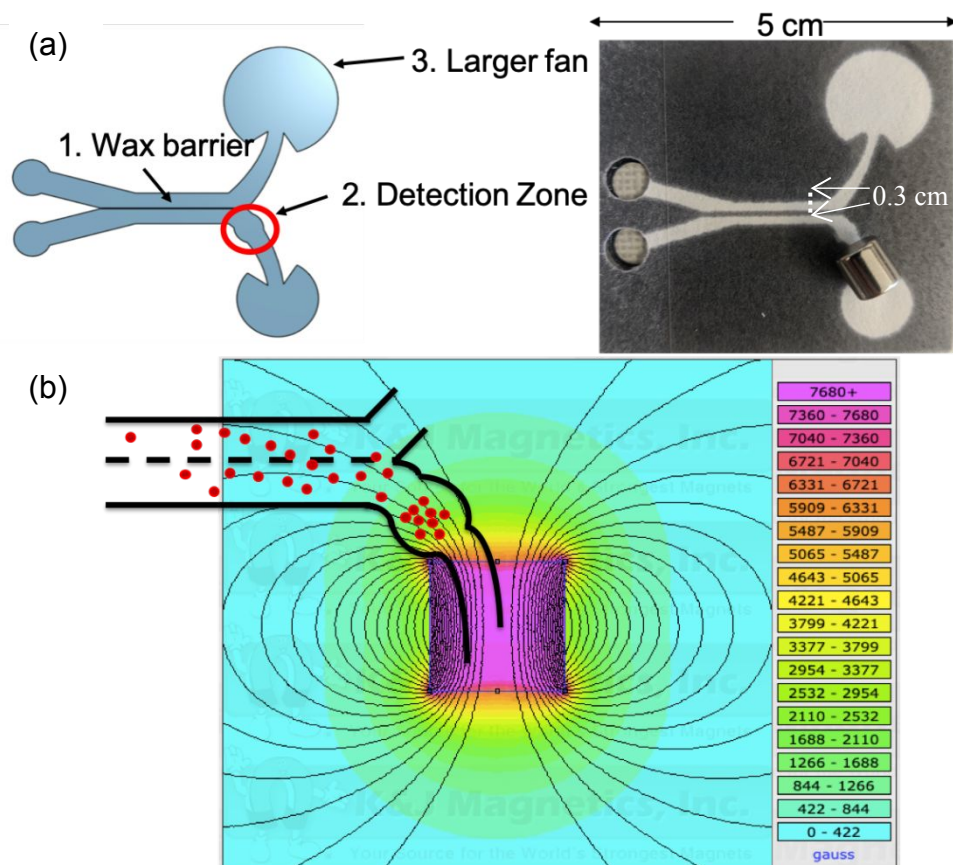
Fig. 5 *(a) CAD rendering of device design and an actual image of the fabricated µPAD. (b) Magnetic field gradient of a N52 cylindrical NdFeB magnet overlay with channel, red spheres indicate magnetic particles. Magnetic flux density estimated to be 1300 guass or 130 mT near the center of the channel. (Magnet image enlarged for viewing purpose)*

3.4 *E. coli* Magnetophoresis in Urine

Escherichia coli (*E. coli*) is a common bacterium found in food and water that causes millions of infections per year in the US. *E. coli* accounts for 70-95% of all urinary tract infections (UTIs).[29] An immunomagnetic sandwich *E. coli* assay in urine was performed to demonstrate the ability to carry out analysis on real samples. To verify that the 44.1 µm beads would capture *E. coli,* the streptavidin coated beads were modified with biotinylated anti-*E.coli* and incubated with 10^7 CFU/mL *E. coli* labeled with a fluorescent secondary antibody. As shown in **Fig. 6c**, fluorescently labeled bacteria are bound to the surface of the magnetic beads at 10^7 CFU/mL. To demonstrate

that the device could process a complex sample matrix, the optimized magnetophoresis assay was performed using human urine. 30 µL of the streptavidin magnetic bead antibody complex was incubated in a urine sample spiked with *E. coli* during the antibody conjugation. A full schematic of the conjugation process can be found in the supporting information. After conjugation was complete, the complex was resuspended in urine and the detection of the labeled *E. coli* was shown in the device via magnetophoresis along with a blank (**Figs. 6a and b)** at 10^7 CFU/mL of *E. coli* for the positive test. Next, serial dilutions from 10^7 CFU/mL to 10^1 CFU/mL were used to create a dose-response curve (**Fig. 6d**). The LOD in the device of 10^5 CFU/mL is not as low as a colorimetric response seen previously by our group of 10^2 CFU/mL for IMS methods,[22] but still demonstrates proof-of-concept. Detection limits could be improved in a few ways. First, enzymatic amplification instead of a fluorescent tag has been shown to improve the LOD especially in µPADs. Second, if the lower concentrations of *E. coli* were cultured prior to conjugation it would improve the LOD as well.[30, 31] The final complex was introduced into the device and compared against the blank to see significant capture *E. coli* in the device in less than 30 s. Further investigation will be done to try to improve the capture efficiency with sequential washing steps to fully wash any complexes left in the inlet, and by adding a surfactant to the buffer to decrease particle-transparency interactions. Fluorescence detection is convenient for rapid detection of the complex, however we found it was limited by intensity when trying to record the entire channel.
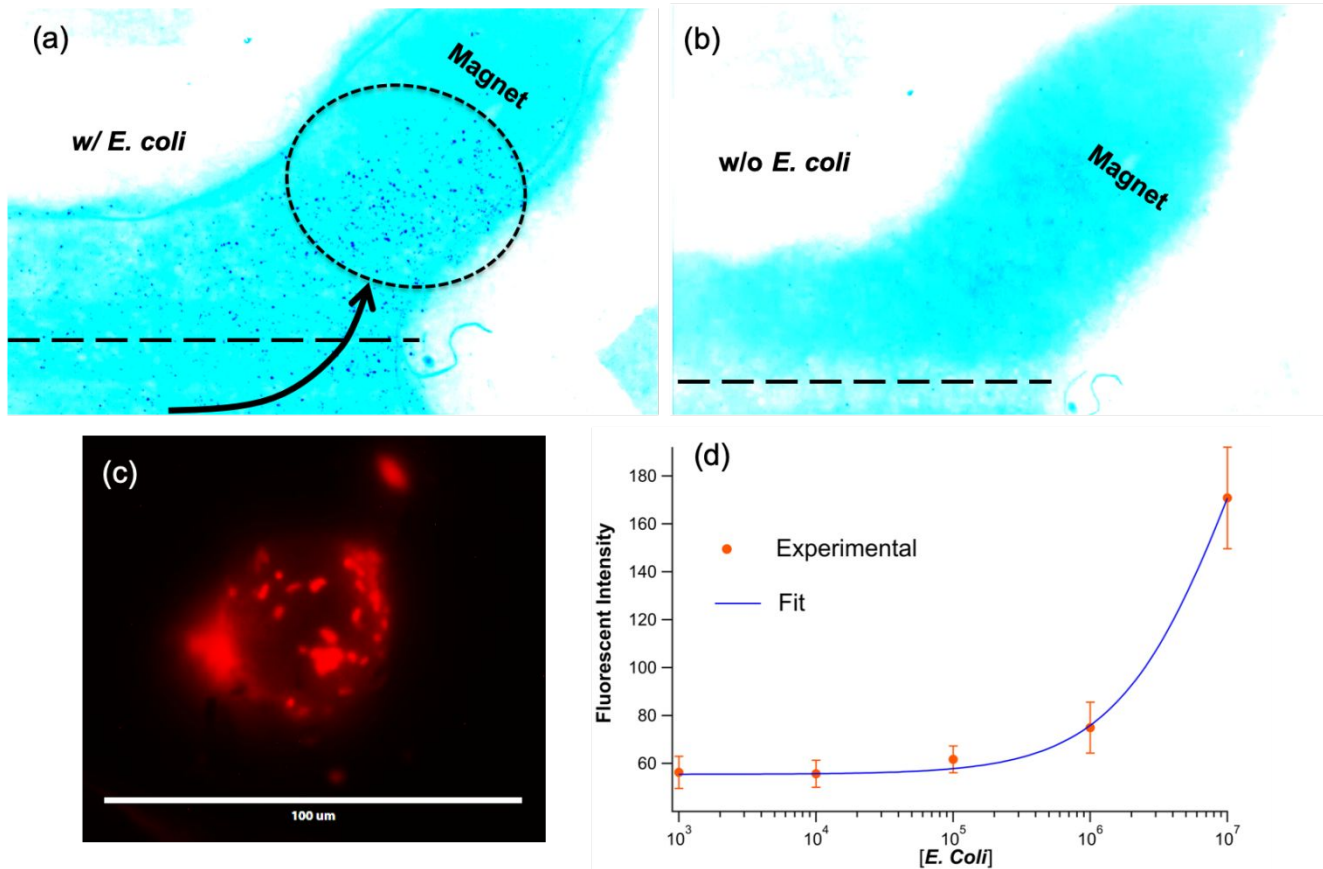
Fig. 6 Detection of fluorescently labeled bacteria in µPAD magnetophoresis. *(a) Inverted image of positive magnetophoresis of E. coli complex. (b) Negative control assay (without E. coli). False color has been applied for visualization (c) Fluorescent microscope image taken of bound E. coli to bead. (d) Dose-response curve of E.coli in urine in the device*

4. Conclusions and Future Directions

In this work, the first example of a pump-free paper-based magnetophoresis device is demonstrated. The novel design shows efficient capture and detection of magnetic particles made possible by the fast flow system with sustained high velocities. Device dimensions, particle size, gap height, and magnet placement and strength were all studied to improve particle capture and reduce convective and diffusional mixing between the two flow streams. A capture efficiency of 61.5% was obtained and further investigation is being done to improve this as described above. Even though this capture efficiency is not as high as other magnetophoretic devices, this device

represents a novel approach to a technique that has not previously been demonstrated in paper. The current method for this assay involves several off-chip steps, but future work will also seek to integrate all steps to minimize assay complexity. We envision additional new potential diagnostic platforms possible because of the technique described. Future work will target adapting the system to incorporate the off-chip manipulations onto the device and to detect multiple pathogens at once.

1
2
3
4
5
6
7
8
9
10
11
12
13
14
15
16
17
18
19
20
21
22
23
24
25
26
27
28
29
30
31
32
33
34
35
36
37
38
39
40
41
42
43
44
45
46
47
48
49
50
51
52
53
54
55
56
57
58
59
60

Supplementary Material

Acknowledgements

References

1.   Dye, C., After 2015: infectious diseases in a new era of health and development. *Philosophical Transactions of the Royal Society B-Biological Sciences* **2014,** *369* (1645).

2.   Carrell, C.; Kava, A.; Nguyen, M.; Menger, R.; Munshi, Z.; Call, Z.; Nussbaum, M.; Henry, C., Beyond the lateral flow assay: A review of paper-based microfluidics. **2019,** *206*, 45-54.

3.   Petryayeva, E.; Algar, W. R., Toward point-of-care diagnostics with consumer electronic devices: the expanding role of nanoparticles. *Rsc Advances* **2015,** *5* (28), 22256-22282.

4.   Martinez, A. W.; Phillips, S. T.; Whitesides, G. M.; Carrilho, E., Diagnostics for the Developing World: Microfluidic Paper-Based Analytical Devices. *Analytical Chemistry* **2010,** *82* (1), 3-10.

5.   Yager, P.; Domingo, G. J.; Gerdes, J., Point-of-care diagnostics for global health. *Annual Review of Biomedical Engineering* **2008,** *10*, 107-144.

6.   Dellinger, R. P.; Levy, M. M.; Rhodes, A.; Annane, D.; Gerlach, H.; Opal, S. M.; Surviving Sepsis Campaign, G., Surviving Sepsis Campaign: International Guidelines for Management of Severe Sepsis and Septic Shock: 2012. *Crit. Care Med.* **2013,** *41* (2), 580-637.

7.   Chin, C. D.; Linder, V.; Sia, S. K., Commercialization of microfluidic point-of-care diagnostic devices. *Lab on a Chip* **2012,** *12* (12), 2118-2134.

8.   Myers, F. B.; Lee, L. P., Innovations in optical microfluidic technologies for point-of-care diagnostics. *Lab on a Chip* **2008,** *8* (12), 2015-2031.

9.   Mahony, J. B.; Blackhouse, G.; Babwah, J.; Smieja, M.; Buracond, S.; Chong, S.; Ciccotelli, W.; O'Shea, T.; Alnakhli, D.; Griffiths-Turner, M.; Goeree, R., Cost Analysis of Multiplex PCR Testing for Diagnosing Respiratory Virus Infections. *Journal of Clinical Microbiology* **2009,** *47* (9), 2812-2817.

10.   Bissonnette, L.; Bergeron, M. G., Diagnosing infections--current and anticipated technologies for point-of-care diagnostics and home-based testing. *Clinical Microbiology and Infection* **2010,** *16* (8), 1044-1053.

11.   Wormser, G. P.; Levin, A.; Soman, S.; Adenikinju, O.; Longo, M. V.; Branda, J. A., Comparative Cost-Effectiveness of Two-Tiered Testing Strategies for Serodiagnosis of Lyme Disease with Noncutaneous Manifestations. *Journal of Clinical Microbiology* **2013,** *51* (12), 4045-4049.

12.   Land, K. J.; Boeras, D. I.; Chen, X.-S.; Ramsay, A. R.; Peeling, R. W., REASSURED diagnostics to inform disease control strategies, strengthen health systems and improve patient outcomes. *Nature Microbiology* **2019,** *4* (1), 46-54.

13.   Osborn, J. L.; Lutz, B.; Fu, E.; Kauffman, P.; Stevens, D. Y.; Yager, P., Microfluidics without pumps: reinventing the T-sensor and H-filter in paper networks. *Lab on a Chip* **2010,** *10* (20), 2659-2665.

14.   Bhagat, A. A. S.; Bow, H.; Hou, H. W.; Tan, S. J.; Han, J.; Lim, C. T., Microfluidics for cell separation. *Medical & Biological Engineering & Computing* **2010,** *48* (10), 999-1014.

15.   Yaman, S.; Anil-Inevi, M.; Ozcivici, E.; Tekin, H. C., Magnetic Force-Based Micro fluidic Techniques for Cellular and Tissue Bioengineering. *Front. Bioeng. Biotechnol.* **2018,** *6*, 29.

16.   Zborowski, M.; Ostera, G. R.; Moore, L. R.; Milliron, S.; Chalmers, J. J.; Schechter, A. N., Red blood cell magnetophoresis. *Biophysical journal* **2003,** *84* (4), 2638-2645.

17.   Cate, D. M.; Adkins, J. A.; Mettakoonpitak, J.; Henry, C. S., Recent Developments in Paper-Based Microfluidic Devices. *Analytical Chemistry* **2015,** *87* (1), 19-41.

18.   Kasetsirikul, S.; Shiddiky, M. J. A.; Nguyen, N.-T., Challenges and perspectives in the development of paper-based lateral flow assays. *Microfluidics and Nanofluidics* **2020,** *24* (2), 17.

19.   Channon, R. B.; Nguyen, M. P.; Scorzelli, A. G.; Henry, E. M.; Volckens, J.; Dandy, D. S.; Henry, C. S., Rapid flow in multilayer microfluidic paper-based analytical devices. *Lab on a Chip* **2018,** *18* (5), 793-802.

20.   Robert B. Channon, M. P. N., Charles S. Henry, David S. Dandy, Multilayered Microfluidic Paper-Based Devices: Characterization, Modeling, and Perspectives. 2019.

21.   Adkins, J. A.; Boehle, K.; Friend, C.; Chamberlain, B.; Bisha, B.; Henry, C. S., Colorimetric and Electrochemical Bacteria Detection Using Printed Paper- and Transparency-Based Analytic Devices. *Analytical Chemistry* **2017,** *89* (6), 3613-3621.

22.   Srisa-Art, M.; Boehle, K. E.; Geiss, B. J.; Henry, C. S., Highly Sensitive Detection of Salmonella typhimurium Using a Colorimetric Paper-Based Analytical Device Coupled with Immunomagnetic Separation. *Analytical Chemistry* **2018,** *90* (1), 1035-1043.

23.   Pamme, N.; Manz, A., On-chip free-flow magnetophoresis: Continuous flow separation of magnetic particles and agglomerates. *Analytical Chemistry* **2004,** *76* (24), 7250-7256.

24.   Choban, E. R.; Markoski, L. J.; Wieckowski, A.; Kenis, P. J. A., Microfluidic fuel cell based on laminar flow. *J. Power Sources* **2004,** *128* (1), 54-60.

25.   Mendez, S.; Fenton, E. M.; Gallegos, G. R.; Petsev, D. N.; Sibbett, S. S.; Stone, H. A.; Zhang, Y.; Lopez, G. P., Imbibition in Porous Membranes of Complex Shape: Quasi-stationary Flow in Thin Rectangular Segments. *Langmuir* **2010,** *26* (2), 1380-1385.

26.   Pamme, N.; Wilhelm, C., Continuous sorting of magnetic cells via on-chip free-flow magnetophoresis. *Lab on a Chip* **2006,** *6* (8), 974-980.

27.   K&J magnetics, I. Magnetic Field Visualization Single Magnet in Free Space. https://www.kjmagnetics.com/magfield.asp?pName=D22-N52 (accessed 01-11-20).

28.   Alnaimat, F.; Dagher, S.; Mathew, B.; Hilal-Alnqbi, A.; Khashan, S., Microfluidics Based Magnetophoresis: A Review. *Chem. Rec.* **2018,** *18* (11), 1596-1612.

29.   Flores-Mireles, A. L.; Walker, J. N.; Caparon, M.; Hultgren, S. J., Urinary tract infections: epidemiology, mechanisms of infection and treatment options. *Nature Reviews Microbiology* **2015,** *13* (5), 269-284.

30.   Shih, C. M.; Chang, C. L.; Hsu, M. Y.; Lin, J. Y.; Kuan, C. M.; Wang, H. K.; Huang, C. T.; Chung, M. C.; Huang, K. C.; Hsu, C. E.; Wang, C. Y.; Shen, Y. C.; Cheng, C. M., Paper-based ELISA to rapidly detect Escherichia coli. *Talanta* **2015,** *145*, 2-5.
31.   Aspevall, O.; Osterman, B.; Dittmer, R.; Stén, L.; Lindbäck, E.; Forsum, U., Performance of Four Chromogenic Urine Culture Media after One or Two Days of Incubation Compared with Reference Media. *Journal of Clinical Microbiology* **2002,** *40* (4), 1500-1503.